Two-photon absorption induced transmission changes in ZnSe interference filters

E. W. Van Stryland, Steven A. Miller,* and M. A. Woodall†

Center for Research in Electro-Optics and Lasers, University of Central Florida, Orlando, Florida 32816

B. S. Wherrett

Department of Physics, Heriot-Watt University, Edinburgh, UK

Received November 12, 1987; accepted February 17, 1988

We observe two-photon absorption (2PA) of picosecond, 0.6-μm, 0.3-nJ pulses in a 0.4-μm film of ZnSe. We use high-frequency-modulation phase-sensitive detection to be near the shot-noise limit combined with a low-frequency pulse-delay modulation to discriminate against large thermal nonlinearities. This dual-modulation technique, combined with the field enhancement produced by placing the film in a resonant cavity, permits observation of 2PA and other fast nonlinearities by using pulses having peak powers of the order of 1 W.

The use of thin films as nonlinear elements in optical devices is gaining considerable attention as interest in optical computing grows. The operation of such thin-film devices is critically dependent on the nonlinear material used for the film. We present here a sensitive method for monitoring a nonlinearly induced transmission change that is particularly useful for observation of fast nonlinearities in thin-film structures. This technique permits assessment of the nonlinearity by using a beam oriented perpendicular to the film surface rather than in the guided-wave geometry.

Using this technique, we observed transmission changes in a probe beam induced by two-photon absorption (2PA) of picosecond 0.6-μm dye laser pulses in a 0.4-μm-thick ZnSe film sandwiched between reflective coatings. These Fabry–Perot structures have been used with cw lasers to demonstrate bistability induced by the slow thermal refractive-index change.[1] In order to observe 2PA in thin films, we use two separate methods to enhance the signal-to-noise ratio. A dual-modulation scheme enhances the sensitivity for observing small transmission changes while discriminating against the large thermal nonlinearities. The Fabry–Perot cavity enhances the irradiance and thus directly increases the transmission change. The results of calculations of the 2PA enhancement in a Fabry–Perot cavity are consistent with experimental results and indicate that a 3-order-of-magnitude enhancement of 2PA is readily obtainable. Combining these two methods, we are able to detect signals so small that they correspond to a calculated single-pass change in transmission of $\sim 10^{-10}$.

The experimental apparatus is shown schematically in Fig. 1. Pulses from a synchronously mode-locked dye laser operating at ~80 MHz, using a three-plate birefringent-filter tuning element, are split into two paths. The excitation beam e reflects off a corner cube mounted on an audio speaker, passes through an electro-optic modulator placed between polarizers to yield a 10-MHz amplitude modulation, and then goes through the sample to a beam block. The probe beam p travels along a variable-delay line through the sample to the detector. The two beams are focused and are overlapped spatially and temporally in the sample. The detector output is sent to a lock-in amplifier referenced to the 10-MHz modulation. The lock-in output is thus proportional to the transmission change induced on beam p by beam e. A similar high-frequency-modulation technique was used previously to yield near-shot-noise-limited detection of other nonlinearities.[2] The method relies on the laser's being noise free near the 10-MHz modulation frequency.

Thermal nonlinearities, often observed when this high-frequency-amplitude-modulation method is used, were eliminated in the past by introducing an additional slow frequency modulation on the excitation beam.[3] The success of that method relies on strong dispersion in the nonlinear response. Since strong dispersion of 2PA in semiconductors occurs only near the band edge,[4] we devised a novel and alternative method for discriminating against thermal nonlinearities. The corner cube mounted on an audio speaker, shown in Fig. 1, induces a slow modulation in the optical path of the excitation beam. This modulation varies the temporal pulse overlap of the beams and thus the total irradiance at the sample. This is accomplished while maintaining constant fluence and average power. By synchronously detecting with a second lock-in at this low frequency, the apparatus is sensitive only to irradiance-dependent processes such as 2PA. The time constant of the first lock-in is set to pass the low-frequency temporal-delay modulation signal. We found this method to be useful for monitoring beam depletion caused by second-harmonic generation, 2PA in bulk samples, saturation phenomena, beam coupling, and Kerr rotation by using appropriate polarizers in the experimental setup. However, the observation of these nonlinearities in thin films requires a higher irradiance to increase the signal above the sensitivity limit of our detection system.

The irradiance is enhanced by placing the ZnSe film be-

0740-3224/88/061289-04$02.00

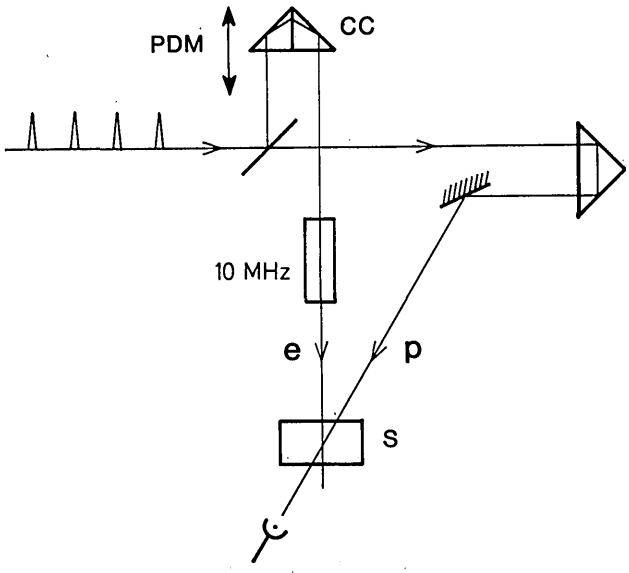

Fig. 1. Dual-modulation experimental setup. A corner cube (CC) is mounted on an audio speaker used for obtaining pulse-delay modulation (PDM); s denotes the sample. The 10-MHz amplitude modulation is provided by an electro-optic modulator placed between polarizers.

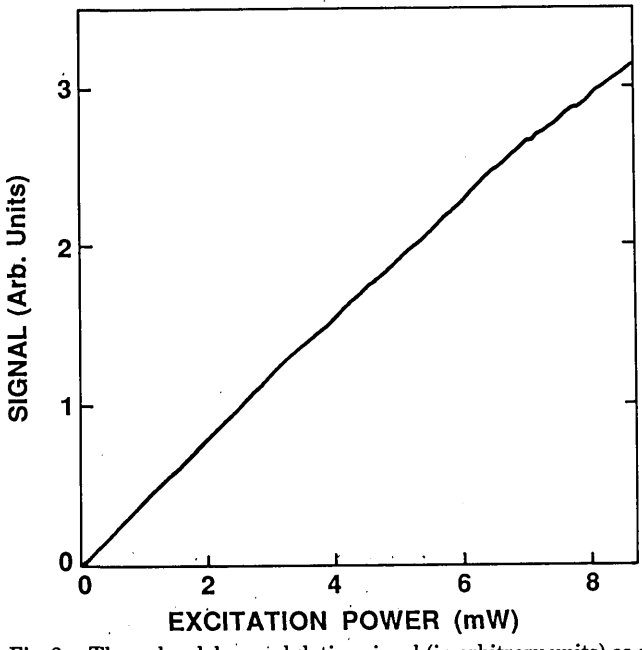

Fig. 2. The pulse-delay modulation signal (in arbitrary units) as a function of the power in the excitation beam.

tween two reflective dielectric stacks, as in a narrow-band interference filter. If linear absorption is ignored, the internal irradiance in the ZnSe spacer layer is increased on resonance by a factor $(1+R)/(1-R)$. Since 2PA is proportional to the square of the internal irradiance, the Fabry–Perot effect can greatly increase the signal (in practice by $\sim 10^3$). The resulting loss is still small enough to permit an analytic solution of the 2PA equations in the small-depletion limit. The result for the induced probe transmission change is derived in Appendix A [Eq. (A9)] to be

$$\Delta T = -2\beta I_e L \frac{1-e^{-\alpha L}}{\alpha L e^{\alpha L}} \times \frac{(1-R_1)^2(1-R_2)(1+R_2e^{-\alpha L})(1+R_\alpha)}{(1-R_\alpha)^5} \tau_p{}^2 \tau_e, \quad (1)$$

where $\tau_{p;e} = (1 + F_\alpha \sin^2 k_{p,e}L)^{-1}$ is the linear-transmission line shape of beam p or e. We verified the predicted linear dependence of the signal on I_e and I_p, although at high

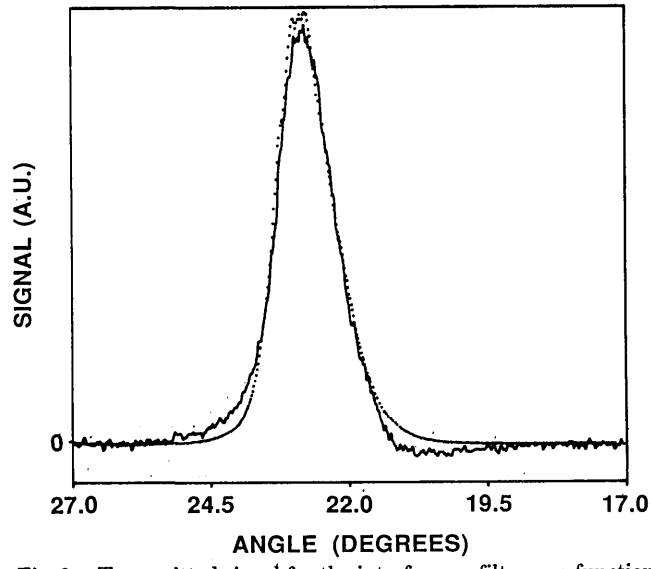

Fig. 3. Transmitted signal for the interference filter as a function of external angle of incidence (α in Fig. 4), for the nonlinear line shape (solid line) and for the cube of the linear line shape (dotted line).

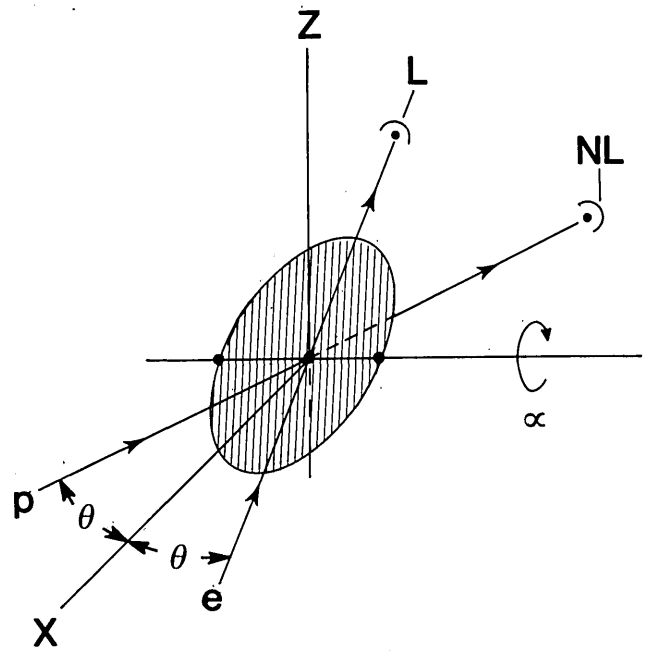

Fig. 4. Geometrical arrangement for measuring the angular dependence of the signal as in Fig. 3. The angle θ for Fig. 3 was fixed at $\sim 6°$, and α was varied. The detectors labeled L and NL indicate that the linear and nonlinear transmitted signals can be monitored simultaneously.

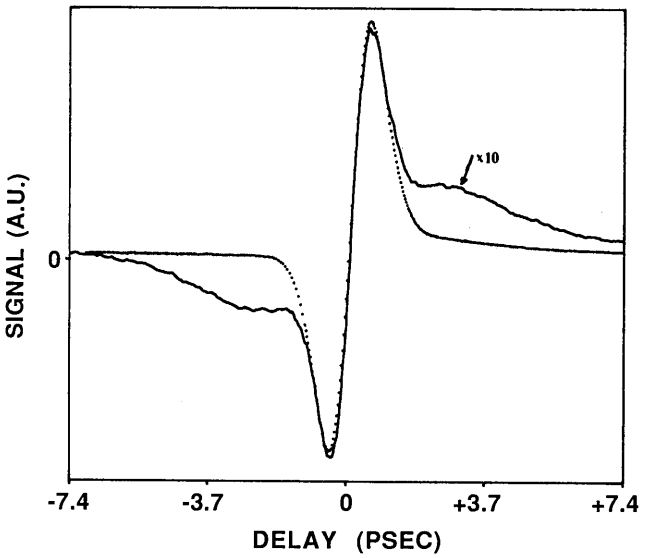

Fig. 5. Pulse-delay modulation signal as a function of time delay between pulses for the bulk ZnSe sample (solid line) and the ZnSe interference filter (dotted line).

inputs a small deviation from linearity was observed, as shown in Fig. 2. This may be due to a slight departure from the small-depletion limit. Given reflectivities $R_1 \simeq R_2 \simeq 0.97$ and losses $\alpha L \simeq 0.01$ that are consistent with the observed linear transmission, we find that $\Delta T \simeq -2000\beta I_e L$. Equation (1) can be verified by monitoring the signal as a function of the angular dependence implicit in $k_{p,e}L$. We determined experimentally that for our beams $\tau_e = \tau_p$, thus Eq. (1) predicts a cubic dependence of ΔT on linear-transmission line shape. Figure 3 shows plots of ΔT (solid line) and the cube of the linear-transmission curve (dotted line) as functions of angle. The geometrical arrangement of the sample for this experiment is shown in Fig. 4. Overlap of the curves in Fig. 3 verifies Eq. (1) and, in addition, shows no shift in resonance peak from nonlinear refraction. At these low irradiance levels the density of photogenerated carriers is expected to be low, keeping this type of nonlinear refraction negligible. Thermally induced nonlinear refraction is present, and, on tight focusing, these filters display bistability.[1] However, we monitored the linear-transmission line shape (angular dependence) for irradiance levels up to a factor of $\simeq 2$ above the level used for Fig. 3 and saw no differences in shape. In addition, this dual-modulation technique is insensitive to such slow cumulative changes in the sample properties.

Irradiance enhancement was verified by comparing the time-delay dependence of the transmission change obtained for the interference filter with that obtained for bulk ZnSe. The interaction length of the beams in the bulk samples was $\simeq 100$ μm. When a small delay modulation ($\simeq 100$ fsec) is used, this signal from a bulk 2PA material is simply proportional to the derivative of the pulse-intensity autocorrelation function. The results of these measurements are shown in Fig. 5 for both the bulk sample (solid line) and the interference filter (dotted line). The bulk signal is magnified by a factor of 10. If the 2PA coefficient for the thermally deposited ZnSe film is assumed to be the same as for bulk ZnSe, Eq. (1) gives, for the ratio of the transmission change for the interference filter ΔT_{IF} to the transmission change for bulk material ΔT_B,

$$\frac{\Delta T_{IF}}{\Delta T_B} = \frac{I_{IF} L_{IF}}{I_B L_B}. \tag{2}$$

Given that the ratio $L_B/L_{IF} \simeq 200$, Eq. (2) gives an estimate of 2000 for the ratio of irradiances I_{IF}/I_B, which is consistent with the irradiance enhancement within the Fabry–Perot cavity as calculated earlier. The exact agreement can only be fortuitous, since the enhancement factor is critically dependent on the reflectances of the dielectric stacks within the interference filter and on the linear-absorption losses in the ZnSe spacer layer, none of which is accurately known. Additionally, the conclusion that the 2PA coefficients for the film and for bulk ZnSe are equal is, at best, true only to within a factor of 2.

The three-plate birefringent filter was misaligned deliberately to give non-bandwidth-limited pulses, and the Fabry–Perot signal in Fig. 5 extends only over the coherence width of the pulses as determined by separate fringe-resolved autocorrelation function measurements.[5] This is expected, since signal enhancement requires mutual coherence of the pulses in both beams. In order for the probe pulse to "see" the field enhancement of the excitation pulse, it must be present in the cavity during the time in which the excitation field is enhanced (i.e., within the coherence time of the probe pulse). This is also necessary for the excitation pulse to "see" the field enhancement of the probe pulse. Thus the 2PA signal is enhanced only when both beams e and p are in the Fabry–Perot cavity within their coherence times, as we observe. The cavity lifetime for the interference filters is $\simeq 100$ fsec, which corresponds to $\simeq 10$ round trips. For the full irradiance enhancement to be realized, the pulses should have a coherence length of several times the cavity lifetime. Our pulses had a coherence time greater than a picosecond.

Although we used these methods to monitor 2PA, they should be applicable for the observation of other nonlinearities. Additionally, these techniques offer interesting new ways to characterize laser pulses.

APPENDIX A

The third-order polarization (P_{n1}) affecting the propagation of the probe beam p (see Fig. 6) in the presence of its reflec-

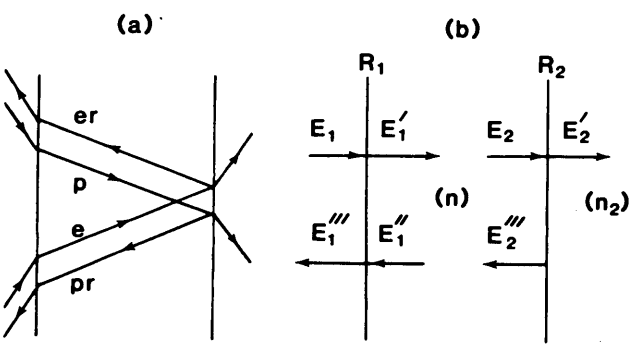

Fig. 6. (a) Fabry–Perot spacer layer, showing the probe and excitation beams along with their reflections. (b) Fields and propagation directions used for calculating Eqs. (A5).

tion (beam pr) and a second excitation beam and its reflection (beams e and er) is given by:

$$P_{\rm nl} = K\epsilon_p(\epsilon_p{}^2 + 2\epsilon_e{}^2 + 2\epsilon_{pr}{}^2 + 2\epsilon_{er}{}^2), \tag{A1}$$

where K is a constant of proportionality. In Eq. (A1) it is assumed that the beams p and e and their reflections are all distinct or that beams p and e have different frequencies. This nonlinear polarization leads to Maxwell's equations, including linear absorption α, given by

$$\frac{1}{\epsilon_p}\frac{\partial\epsilon_p}{\partial z} = -\frac{\alpha}{2} - K[\epsilon_p{}^2 + 2\epsilon_e{}^2 + 2\epsilon_{pr}{}^2 + 2\epsilon_{er}{}^2], \tag{A2a}$$

$$\frac{1}{\epsilon_{pr}}\frac{\partial\epsilon_{pr}}{\partial z} = \frac{\alpha}{2} + K[\epsilon_{pr}{}^2 + 2\epsilon_{er}{}^2 + 2\epsilon_p{}^2 + 2\epsilon_e{}^2], \tag{A2b}$$

along with similar equations for beams e and er. Here, the equations are written for normal incidence such that beams p and pr are counterpropagating. Under the assumption that the nonlinear losses are small, appropriate for our experimental conditions, Equations (A2) can be solved to give the total fields $E_{\rm p,pr}$:

$$E_p(z) = \epsilon_p(0)\exp\left[\left(ik_p - \frac{\alpha}{2} - \frac{\beta_1}{2}\right)z\right],$$

$$E_{pr}(z) = \epsilon_{pr}(0)\exp\left[\left(-ik_p + \frac{\alpha}{2} + \frac{\beta_2}{2}\right)z\right], \tag{A3}$$

where k_p is the propagation constant of beam p and β_1 and β_2 are the spatial averages (taking into account linear losses) of the bracketed portions of Eqs. (A2); that is,

$$\beta_1 = \frac{K(1-e^{-\alpha L})}{\alpha L}\{\epsilon_p{}^2(0) + 2\epsilon_e{}^2(0) + 2[\epsilon_{pr}{}^2(0) + \epsilon_{er}{}^2(0)]e^{\alpha L}\}, \tag{A4a}$$

$$\beta_2 = \frac{K(1-e^{-\alpha L})}{\alpha L}\{[\epsilon_{pr}{}^2(0) + 2\epsilon_{er}{}^2(0)]e^{\alpha L} + 2\epsilon_p{}^2(0) + 2\epsilon_e{}^2(0)\}. \tag{A4b}$$

From the boundary conditions imposed on the Fabry–Perot cavity, we can solve for the field ratios in the presence of 2PA. Using the notation of Fig. 6(b), where $E_2 = XE_1'$ and $E_1'' = X_rE_2'''$, with X and X_r given by the respective exponentials in Eqs. (A3) evaluated at $z = L$, we find

$$\frac{E_1'}{E_1} = \frac{1}{D}\left(\frac{1-R_1}{n}\right)^{1/2}, \qquad \frac{E_1''}{E_1} = \frac{XX_r}{D}\left[\frac{R_2(1-R_1)}{n}\right]^{1/2},$$

$$\frac{E_2'}{E_1} = \frac{X}{D}\left[\frac{(1-R_1)(1-R_2)}{n_2}\right]^{1/2}, \qquad \frac{E_2}{E_1} = \frac{X}{D}\left(\frac{1-R_1}{n}\right)^{1/2},$$

$$\frac{E_2'''}{E_1} = \frac{X}{D}\left[\frac{R_2(1-R_1)}{n}\right]^{1/2},$$

$$\frac{E_1'''}{E_1} = \frac{1}{D}[XX_r(R_2)^{1/2} - (R_1)^{1/2}], \tag{A5}$$

where $D = 1 - XX_r(R_1R_2)^{1/2}$. This yields, for the transmitted irradiance I_T in terms of the incident irradiance I_p,

$$I_T = I_p n_2\left|\frac{E_2'}{E_1}\right|^2 = I_p(1-R_1)(1-R_2)\left|\frac{X}{D}\right|^2. \tag{A6}$$

Expanding the exponentials in β_i to first order gives

$$I_T = I_p\left[\frac{(1-R_1)(1-R_2)e^{-\alpha L}}{(1-R_\alpha)^2(1+F_\alpha\sin^2 k_pL)}\right] \times\left\{1 - \beta_1 L - (\beta_1+\beta_2)LR_\alpha\frac{[1-R_\alpha-2\sin^2 k_pL]}{(1-R_\alpha)^2(1\,F_\alpha\sin^2 k_pL)}\right\}, \tag{A7}$$

where $F_\alpha = 4R_\alpha/(1-R_\alpha)^2$ and $R_\alpha = (R_1R_2)^{1/2}e^{-\alpha L}$. Equations (A5) also give the values for β_i in terms of the input irradiance:

$$\beta_1 = \frac{\beta(1-R_1)}{(1-R_\alpha)^2}\frac{1-e^{-\alpha L}}{\alpha L} \times[I_p(1+2R_2e^{-\alpha L})\tau_p + 2I_e(1+R_2e^{-\alpha L})\tau_e], \tag{A8a}$$

$$\beta_2 = \frac{\beta(1-R_1)}{(1-R_\alpha)^2}\frac{1-e^{-\alpha L}}{\alpha L} \times[I_p(2+R_2e^{-\alpha L})\tau_p + 2I_e(1+R_2e^{-\alpha L})\tau_e], \tag{A8b}$$

where $\tau_{p,e} = (1 + F_\alpha\sin^2 k_{p,e}L)^{-1}$ and β is the 2PA coefficient. Higher-order effects of 2PA are neglected in Eqs. (A8). Inserting Eqs. (A8) into Eq. (A7) and keeping only the terms proportional to the product of I_p and I_e gives the change in the probe irradiance ΔI_p induced by the excitation beam. Experimentally, this is proportional to the signal passed by the lock-in amplifier. The signal is thus proportional to

$$\Delta I_p = -I_p 2\beta I_e L\frac{1-e^{-\alpha L}}{\alpha L e^{\alpha L}} \times\frac{(1-R_1)^2(1-R_2)(1+R_2e^{-\alpha L})(1+R_\alpha)}{(1-R_\alpha)^5}\tau_p{}^2\tau_e. \tag{A9}$$

ACKNOWLEDGMENT

We gratefully acknowledge the support of the National Science Foundation (grants ECS-8310625 and ECS-8617066).

* Present address, Department of Physics, North Texas State University, Denton, Texas 76203.

† Present address, Optic-Electronic, 11545 Pagemill Road, Dallas, Texas 75243.

REFERENCES

1. F. V. Karpushko and G. V. Sinitsyn, J. Appl. Spectrosk. (USSR) **29**, 1323 (1978); see also S. D. Smith, J. G. H. Mathew, M. R. Taghizadeh, A. C. Walker, B. S. Wherrett, and A. Hendry, Opt. Commun. **51**, 357 (1984).
2. B. F. Levine and C. G. Bethea, Appl Phys. Lett. **36**, 245 (1980).
3. B. F. Levine, C. V. Shank, and J. P. Heritage, IEEE J. Quantum Electron. **QE-15**, 1418 (1979).
4. E. W. Van Stryland, H. Vanherzeele, M. A. Woodall, M. J. Soileau, A. L. Smirl, S. Guha, and T. F. Boggess, Opt. Eng. **24**, 613 (1985).
5. J.-C. Diels, E. W. Van Stryland, and G. Benedict, Opt. Commun. **25**, 93 (1979); J.-C. Diels, E. W. Van Stryland, and D. Gold, in *Picosecond Phenomena*, C. V. Shank, E. P. Ippen, and S. L. Shapiro, eds. (Springer-Verlag, Berlin, 1978), pp. 117–128.